Submicron Void Formation in Amorphous NiZr Alloys

K. N. Tu and T. C. Chou
IBM Research Division, Thomas J. Watson Research Center, Yorktown Heights, New York 10598
(Received 3 December 1987)

A trilayer thin film of amorphous alloys $Ni_{40}Zr_{60}/Ni_{73}Zr_{27}/Ni_{40}Zr_{60}$ has been deposited on nitrided Si surface, annealed at 200, 250, and 300 °C in He, and analyzed by Rutherford backscattering spectroscopy and cross-sectional transmission electron microscopy. Interdiffusion occurred without crystalization. When Ni was the dominant diffusing species, no voids were seen. When both Ni and Zr diffuse, submicron size voids were observed. This indicates that self-diffusion in the amorphous alloy can be mediated by localized vacancylike defects as well as by nonlocalized free-volume defects. Void formation as a result of the slower diffusing species is opposite to the Kirkendall effect in crystalline solids.

PACS numbers: 66.30.Fq, 61.40.+b, 68.65.+g

Interdiffusion in certain bilayer and multilayer thin-film structures has been shown to lead to amorphous alloy formation. Examples are Rh/Si,[1] La/Au,[2] Ni/Zr,[3,4] Co/Zr,[5] and Ti/Si[6] thin-film couples. Since amorphous alloys do not exist in equilibrium phase diagrams, their formation by interdiffusion, which is a slow heating process, is a kinetic phenomenon. This destruction of long-range order with neither melting nor abrupt energy change is currently the most challenging kinetic issue in solid-state transformation.

Interdiffusion in a layered structure requires a long-range diffusion across a concentration gradient, so the amorphous alloy formed by solid-state reaction must be able to exist over a wide composition range in order to sustain the gradient and must allow long-range diffusion (rather than short-range relaxation) to occur without crystallization. Crystallization transforms the amorphous alloy and requires the nucleation of a crystalline phase. The metastability of the amorphous alloy formed by interdiffusion, therefore, relies on a rather stable structure which tolerates a large flow of atomic fluxes and has a high nucleation barrier for the crystalline phase. Obviously, structural defects are of concern.

The occurrence of a long-range diffusion in an amorphous alloy depends on the mechanism of diffusion. Long-range diffusion in homogeneous amorphous alloys has been demonstrated by tracer diffusion of radioactive Ag in an amorphous $Pd_{81}Si_{19}$ alloy.[7] Long-range diffusion in inhomogeneous amorphous alloys occurs during their formation by interdiffusion. Since a lattice, and in turn, a lattice defect such as a vacant site, cannot be defined in an amorphous solid, the concept of free volume, which is not a localized defect, has been proposed to mediate diffusion in amorphous solids.[8,9] Recently, a defect of complex and many-body nature has also been proposed for diffusion of Ag and Au in amorphous CuZr alloys.[10] Their diffusion is characterized by having a lower activation energy but a larger and negative entropy factor than those in crystals such as Cu. Still, the atomistic picture of diffusion and the defect which mediates diffusion in an amorphous alloy are far from clear.

In the case of interdiffusion in Ni/Zr bilayers, the amorphous alloy formed has a concentration gradient which goes from about $Ni_{47}Zr_{53}$ to $Ni_{68}Zr_{32}$ over a thickness of several hundred angstroms[11]; Ni is the dominant diffusing species,[12] and voids form in the Ni layer neighboring the interface between the Ni and the amorphous alloy.[4] Voids have not been found in the amorphous alloy nor in the Zr layer. The void formation tends to indicate that Ni diffuses via defects rather than by a direct exchange with neighboring atoms or by a rotation of a cluster of atoms. It has been shown that Ni diffuses rapidly in Zr,[13] similar to Au in Pb. This has raised the possibility that the diffusing Ni atoms could enter interstitially into the amorphous alloy and the vacant sites they leave behind in the Ni lattice form voids. The Ni atoms could diffuse into the alloy by exchanging with nonlocalized free-volume defects and the defects must collapse quickly since the surface of the amorphous alloy appears smooth and free of dimples due to condensation of the defects as viewed by cross-sectional transmission electron microscopy. We note that in interdiffusion between Ni and Zr, no significant Zr diffusion has been observed. In this Letter, we report the results of interdiffusion between couples of amorphous NiZr alloys, with no crystalline phases. We have forced Zr atoms to diffuse in order to reveal the defect picture.

A trilayer thin-film structure of amorphous alloys consisting of 725-Å $Ni_{40}Zr_{60}$/1500-Å $Ni_{73}Zr_{27}$/630-Å $Ni_{40}Zr_{60}$ was prepared by electron-beam coevaporation onto nitrided, (100) oriented Si wafers. The wafers were water cooled during alloy deposition in vacuum of low 10^{-7} Torr. After the deposition the wafer was diced into 1-cm^2 pieces for annealing at 200, 250, and 300 °C for up to 24 h in a quartz tube furnace flooded with He gas purified by passing through a Ti filter kept at 950 °C. The samples were analyzed by Rutherford backscattering spectroscopy (RBS) and cross-sectional transmission electron microscopy (TEM) for in-depth compositional

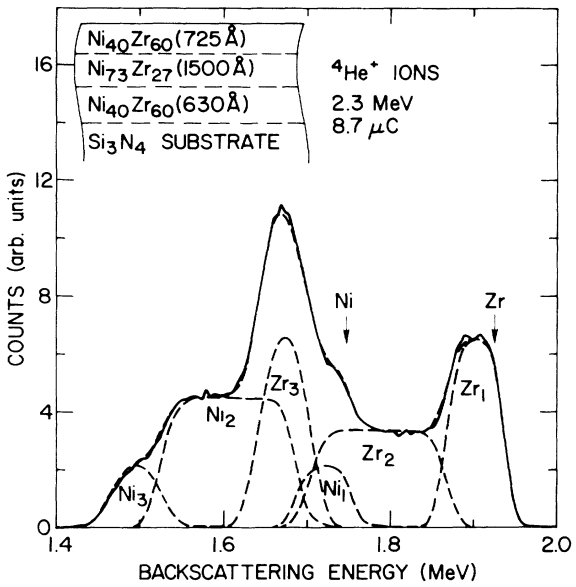

FIG. 1. RBS spectra of the as-deposited trilayer structure. The experimental spectrum is shown as the solid line. The theoretical component spectra of Ni and Zr in each of the trilayers (labeled 1, 2, and 3) are shown as broken lines.

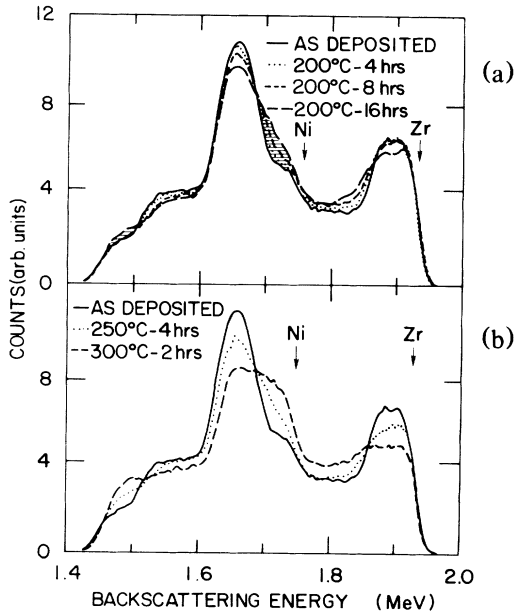

FIG. 2. (a) RBS spectra of a trilayer sample before (solid line) and after annealing at 200 °C for 4 h (dotted line), 8 h (short broken line), and 16 h (long broken line). (b) RBS spectra of a trilayer sample before (solid line) and after annealing at 250 °C for 4 h (dotted line) and at 300 °C for 2 h (broken line).

and morphological changes, respectively. Structural stability was monitored by grazing-incidence x-ray diffraction, transmission electron diffraction, and *in situ* resistivity measurement.

Figure 1 shows the experimental 2.3-MeV $^4He^+$ RBS spectrum (solid line) of the as-deposited trilayer structure, superimposed with a theoretical spectrum (broken line) assuming a structure of 725-Å $Ni_{40}Zr_{60}$/1500-Å $Ni_{73}Zr_{27}$/630-Å $Ni_{40}Zr_{60}$. The theoretical component spectra of Ni and Zr in each of the layers (labeled, 1, 2, and 3) are indicated in the figure. Since the signals of Ni and Zr overlap each other in the energy range of 1.6 to 1.8 MeV, it is convenient to examine the unoverlapped regions of 1.4 to 1.6 MeV and 1.8 to 2.0 MeV for changes in Ni and Zr, respectively, due to annealing.

In the as-deposited state, the trilayer is amorphous with an average resistivity of 210 ± 10 $\mu\Omega$-cm at room temperature. The cross-sectional image in bright-field TEM is featureless. The electron diffraction pattern revealed halos only. X-ray diffraction spectra of samples before and after the annealings showed no sharp reflections. *In situ* isothermal resistivity measurements at the three annealing temperatures up to 12 h revealed no abrupt changes due to phase transformation. On the other hand, compositional and morphological changes have been observed by RBS and cross-sectional TEM, respectively.

Figure 2(a) shows the RBS spectra of samples before (solid line) and after annealing at 200 °C for 4 h (dotted line), for 8 h (short broken line), and for 16 h (long broken line). By comparing them, it can be seen that the concentration of Ni in the side layers has increased from 40% to 43% after the 8-h annealing (as indicated by the shaded areas), yet no Zr diffusion is seen after the 8-h annealing, and there is only a small amount of Zr diffusion seen after the 16-h annealing. This indicates that Ni diffuses predominantly at 200 °C, and a diffusivity of 10^{-14} to 10^{-15} cm^2/sec can be estimated by applying Fick's first law of diffusion. Figure 2(b) shows the RBS spectra of samples as-deposited (solid line), annealed at 250 °C for 4 h (dotted line), and annealed at 300 °C for 2 h (broken line). After the 250 °C annealing, the side layers had a concentration of about 48 at.% Ni and 52 at.% Zr; redistribution of both Ni and Zr had taken place. Specifically, the intensity of the Zr signal at the front end (around 1.9 MeV) decreased, indicating a loss of Zr. Such a change cannot come from the out diffusion of Ni from the middle layer to the outer layer alone; that may have changed the composition in the outer layer but not the amount of Zr. For example, in the case of annealing at 200 °C for 8 h, a substantial diffusion of Ni has occurred, yet the signal of Zr in the outer layer (the front end) did not change [see Fig. 2(a)]. The oxidation of Zr will reduce the signal, yet we should have observed a step rather than the gradual change in the Zr signal. After the 300 °C annealing, the sample was close to homogeneous as shown in Fig. 2(b). We note that this finding agrees with the earlier observation by Hahn, Averback, and Rothman[14] that their diffusion couple of amorphous alloys of $Ni_{33}Zr_{67}$/$Ni_{61}Zr_{39}$ embedded with a diffusion marker of Au was

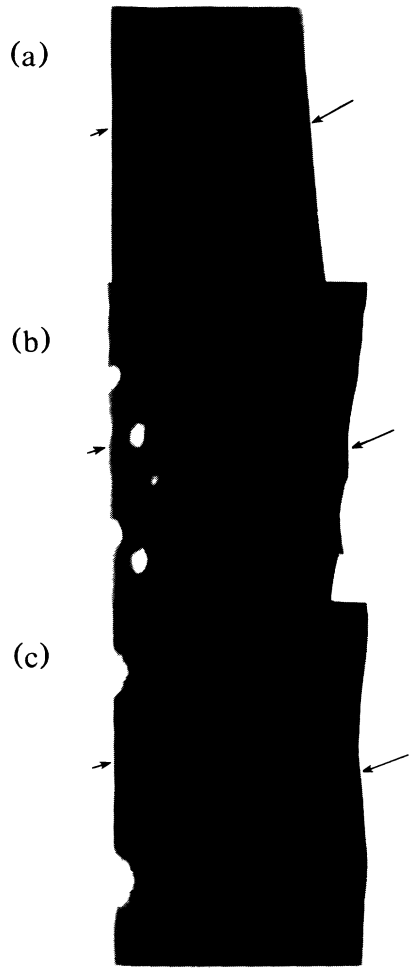

FIG. 3. Cross-sectional bright-field TEM images of annealed trilayer samples (a) at 200 °C for 16 h, (b) at 250 °C for 6 h, and (c) at 300 °C for 2 h. The trilayer film had a thickness of 2850 Å. The long arrows indicate the film surface and the short arrows indicate the substrate interfaces. The variation in film thickness among the three images is due to the difference in magnification.

nearly homogeneous after an anneal at 573 K.

Cross-sectional bright-field TEM images of the samples annealed at 200 °C for 16 h, 250 °C for 6 h, and 300 °C for 2 h are shown in Figs. 3(a), 3(b), and 3(c), respectively. In Fig. 3(a) the image of the trilayer is featureless and is similar to the as-deposited state; no voids are seen, and the surface, as indicated by the long arrows, is smooth and flat. In Fig. 3(b) voids (about 200 Å in size) are seen in the inner layer and also at the film-to-substrate interface, as indicated by the short arrows; the surface appears rough, and the matrix is still featureless. Similar voids were seen in a sample annealed at 250 °C for 1 h. In Fig. 3(c) there are voids at the film-to-substrate interface, but no voids can be found within the film. The surface is smoother than that shown in Fig. 3(b) and the matrix again appears featureless.

To summarize, we found no voids when Ni is the dominant diffusing species, but voids were found when a large flux of Zr diffuses. The finding that Ni diffusion alone produces no voids is consistent with the earlier observation that voids formed in the Ni layer but not in the amorphous layer during the reaction between pure Ni and Zr. Together they indicate that the defect mechanism of Ni diffusion in the amorphous alloy is mediated by nonlocalized free-volume defects whose lifetime at a given location is so short that the structure around the defect collapses and dissipates before a number of them can condense into a void. If we assume that Ni diffuses interstitially in the Ni-rich amorphous alloy, we expect to see voids in the middle layer of the trilayer sample (as we have seen voids in the Ni layer during the reaction between pure Ni and Zr), otherwise the atomic volume left behind by each of the diffusing Ni atoms must have collapsed quickly, and then in essence there is no difference from the free-volume model. Furthermore, we have observed that the Ni diffusion started around 200 °C and Zr diffusion around 250 °C. This indicates that the activation energy of Zr diffusion is comparable to that (1.2 to 1.4 eV) of Ni diffusion since the diffusion process is thermally activated. Then, in a randomly close-packed alloy of Ni-Zr, if Ni diffuses interstitially, we would not expect Zr to diffuse the same within such a close temperature range.

However, the evidence for a localized vacancylike defect mechanism of diffusion in the amorphous NiZr alloy is the voids seen upon Zr diffusion. The atomic volume (or free volume) which exchanges with the Zr atom must be sufficiently large and have a long lifetime to achieve supersaturation so that nucleation and growth of a void can take place. Since Zr is the slower diffusing species in the alloy, the void formation due to Zr diffusion is opposite to the Kirkendall effect in diffusion couples of crystalline solids. The indication is that if we perform marker analysis of a diffusion couple of amorphous NiZr alloys, the flux equation in Darken's analysis must be reconsidered.[15-17] In the crystalline couple of elements A and B, it has been assumed that

$$j_A + j_B + j_V = 0, \tag{1}$$

where the net atomic flux, $j_A + j_B$, is balanced by the vacancy flux, j_V. In the amorphous couple, we might assume two types of free volumes: one for the Ni subnet and the other for the Zr subnet. The latter will play a key role in the analysis, which should be studied carefully by measuring the void volume with respect to marker displacement as a function of time and temperature.

The void formation shows that the metastability of the amorphous alloy not only can withstand a large diffusional flux but also can allow a void surface to be nucleated within the alloy. Clearly nucleation is an issue here,[18] and an important kinetic reason for the solid-

state reaction to form amorphous alloys and for homogenization to occur in an inhomogeneous amorphous alloy without crystallization is the high barrier to heterogeneous crystal nucleation, i.e., a high interfacial energy. Furthermore, the fact that the heat of crystallization is typically small[19,20] (about 1 to 2 kcal/mole for the NiZr alloy) is also helpful in reducing the driving force of crystallization.

The voids seen are not spherical, rather they appear sheared. It would be interesting to investigate the dynamics of these voids upon annealing to see whether they would disappear by relaxation or whether some of them might grow by Ostwald ripening. A quantitative measurement of Zr diffusion in the alloy would also be interesting, especially the preexponential factor which might provide further understanding about the localized defects.

The authors are grateful to R. Petkie for deposition of the amorphous alloy films, P. Saunders for RBS analysis, and R. D. Thompson for assistance in x-ray diffraction.

[1]S. R. Herd, K. N. Tu, and K. Y. Ahn, Appl. Phys. Lett. **42**, 597 (1983).

[2]R. B. Schwartz and W. L. Johnson, Phys. Rev. Lett. **51**, 415 (1983).

[3]B. M. Clemens, W. L. Johnson, and R. B. Schwartz, J. Non-Cryst. Solids **61&62**, 817 (1984).

[4]S. B. Newcomb and K. N. Tu, Appl. Phys. Lett. **48**, 1436 (1986).

[5]H. Schroder, K. Samwer, and U. Koster, Phys. Rev. Lett. **54**, 197 (1985).

[6]K. Holloway and R. Sinclair, J. Appl. Phys. **61**, 1359 (1987).

[7]D. Gupta, K. N. Tu, and K. W. Asai, Phys. Rev. Lett. **35**, 796 (1975).

[8]M. H. Cohen and D. Turnbull, J. Chem. Phys. **31**, 1164 (1959).

[9]D. Turnbull and M. H. Cohen, J. Chem. Phys. **34**, 120 (1960).

[10]D. Lazarus, in *Phase Transitions in Condensed Systems —Experiments and Theory,* edited by G. S. Cargill, III, F. Spaepen, and K. N. Tu, MRS Symposium Proceedings No. 57 (Materials Research Society, Pittsburgh, 1987), p. 297.

[11]J. C. Barbour, Phys. Rev. Lett. **55**, 2872 (1985).

[12]Y. T. Cheng, W. L. Johnson, and M. A. Nicolet, Appl. Phys. Lett. **47**, 800 (1985).

[13]G. M. Hood and R. J. Schultz, Philos. Mag. **26**, 329 (1972).

[14]H. Hahn, R. S. Averback, and S. J. Rothman, Phys. Rev. B **33**, 8825 (1986).

[15]L. Darken, Trans. Am. Inst. Min. Metall. Pet. Eng. **174**, 184 (1948).

[16]J. Bardeen, Phys. Rev. **76**, 1403 (1949).

[17]J. Tardy and K. N. Tu, Phys. Rev. B **32**, 2070 (1985).

[18]A. M. Vredenberg, J. F. M. Westendrop, F. W. Saris, N. M. van der Pers, and Th. H. de Keijser, J. Mater. Res. **1**, 774 (1986).

[19]P. Nash and C. S. Jarjanth, Bull. Alloy Phase Diagrams **5**, 144 (1984).

[20]C. G. McKamey, D. M. Kroeger, D. S. Easton, and J. O. Scarbrough, J. Mater. Sci. **21**, 3862 (1986).

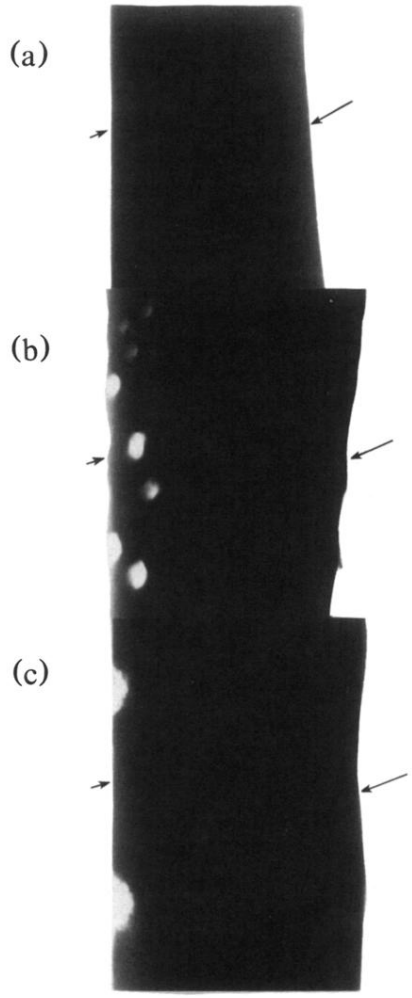

FIG. 3. Cross-sectional bright-field TEM images of annealed trilayer samples (a) at 200 °C for 16 h, (b) at 250 °C for 6 h, and (c) at 300 °C for 2 h. The trilayer film had a thickness of 2850 Å. The long arrows indicate the film surface and the short arrows indicate the substrate interfaces. The variation in film thickness among the three images is due to the difference in magnification.